

Supporting Information

Contents

Fitting Information

Figure S1. Ultrafast XANES difference signals

Table S1. Tabulated energies and oscillator strengths from TDDFT UV-visible absorption calculations for $[\text{Cu(I)(dmp)}_2]^+$ in its ground state geometry

Table S2. Tabulated energies and oscillator strengths from TDDFT UV-visible absorption calculations for $[\text{Cu(I)(dmp)}_2]^+$ in its flattened geometry

Table S3. Tabulated energies and oscillator strengths from TDDFT UV-visible absorption calculations for $[\text{Cu(I)(dmp)}_2]^+$ when flattened by five degrees from the ground state geometry

Table S4. Tabulated energies and oscillator strengths from TDDFT UV-visible absorption calculations for $[\text{Cu(I)(dpps)}_2]^+$ in its ground state geometry

Table S5. Tabulated energies and oscillator strengths from TDDFT UV-visible absorption calculations for $[\text{Cu(I)(dpps)}_2]^+$ in its lowest triplet state geometry

Fitting Information

Pump-probe delay scans were performed at the X-ray photon energy near the 1s - 4p transition that showed the largest signal amplitude in the XANES difference spectra. For both complexes, the resulting traces were fit to a Gaussian instrument response function (IRF) convoluted with a single exponential decay and exponential rise to give $s_r(t)$ in the following:

$$\begin{aligned} \text{IRF}(t) &= e^{-t^2/2\sigma^2}, \quad \Delta A_r(t) = \theta(t) \cdot (1 - e^{-t/\tau_r}) \cdot e^{-t/\tau} \\ s_r(t) &= \int_{-\infty}^{\infty} \exp\left(\frac{-(t-t')^2}{2\sigma^2}\right) \cdot \theta(t') \cdot (1 - e^{-t'/\tau_r}) \cdot e^{-t'/\tau} dt' \\ s_r(t) &= C_r \cdot \exp\left(\frac{\sigma^2}{2\tau^2} - \frac{t}{\tau} - \frac{t}{\tau_r}\right) \\ &\quad \cdot \left[e^{t/\tau_r} \cdot \left(1 - \text{erf}\left(\frac{\sigma^2 - \tau t}{\sqrt{2}\sigma\tau}\right)\right) - \exp\left(\frac{\sigma^2(2\tau_r + \tau)}{2\tau\tau_r^2}\right) \left(1 - \text{erf}\left(\frac{\tau_r\sigma^2 - \tau\tau_r t + \sigma^2\tau}{\sqrt{2}\tau\tau_r\sigma}\right)\right) \right] \end{aligned}$$

Here $\theta(t)$ is a Heaviside step function at time zero. Time zero was included as a fit parameter to correct for small experimental errors (<1 ps) in laser/X-ray pulse timing. Along with the rise and decay constants τ_r and τ , a scaling factor C_r was also varied in the fit. The width of the IRF was allowed to vary in the fit for $[\text{Cu(I)(dmp)}_2]^+$ and was found to be 323 ± 35 fs, confirming the estimated time resolution of ~ 300 fs. This time resolution is likely due to the stochastic nature of the XFEL pulse energy distribution accompanied by a temporal jitter. Also, X-ray and optical pulses experience different indices of refraction in solvent, estimated at 1 fs per μm traveled in our 100 μm diameter jet. Notably, the quality of the fit for $[\text{Cu(I)(dmp)}_2]^+$ was not greatly altered if the rise time (τ_r) was fixed to 10 fs, further suggesting the initial kinetics of the complex are impulsive. The same cannot be said for $[\text{Cu(I)(dpps)}_2]^+$. The slow time component (τ) was found to be 213 ± 37 ps for $[\text{Cu(I)(dmp)}_2]^+$ and much larger than 5 ps for $[\text{Cu(I)(dpps)}_2]^+$. No time component around 200 ps has been previously observed for $[\text{Cu(I)(dmp)}_2]^+$, but, as noted in the main text, the scan times (20 ps for $[\text{Cu(I)(dmp)}_2]^+$ and 5 ps $[\text{Cu(I)(dpps)}_2]^+$) are not long enough to accurately determine the long nanosecond scale ground state recovery recorded for the two complexes.

Figure S1. Ultrafast XANES difference spectra taken from **Figure 4** for $[\text{Cu(I)(dmp)}_2]^+$ (a) and $[\text{Cu(I)(dpps)}_2]^+$ (b).

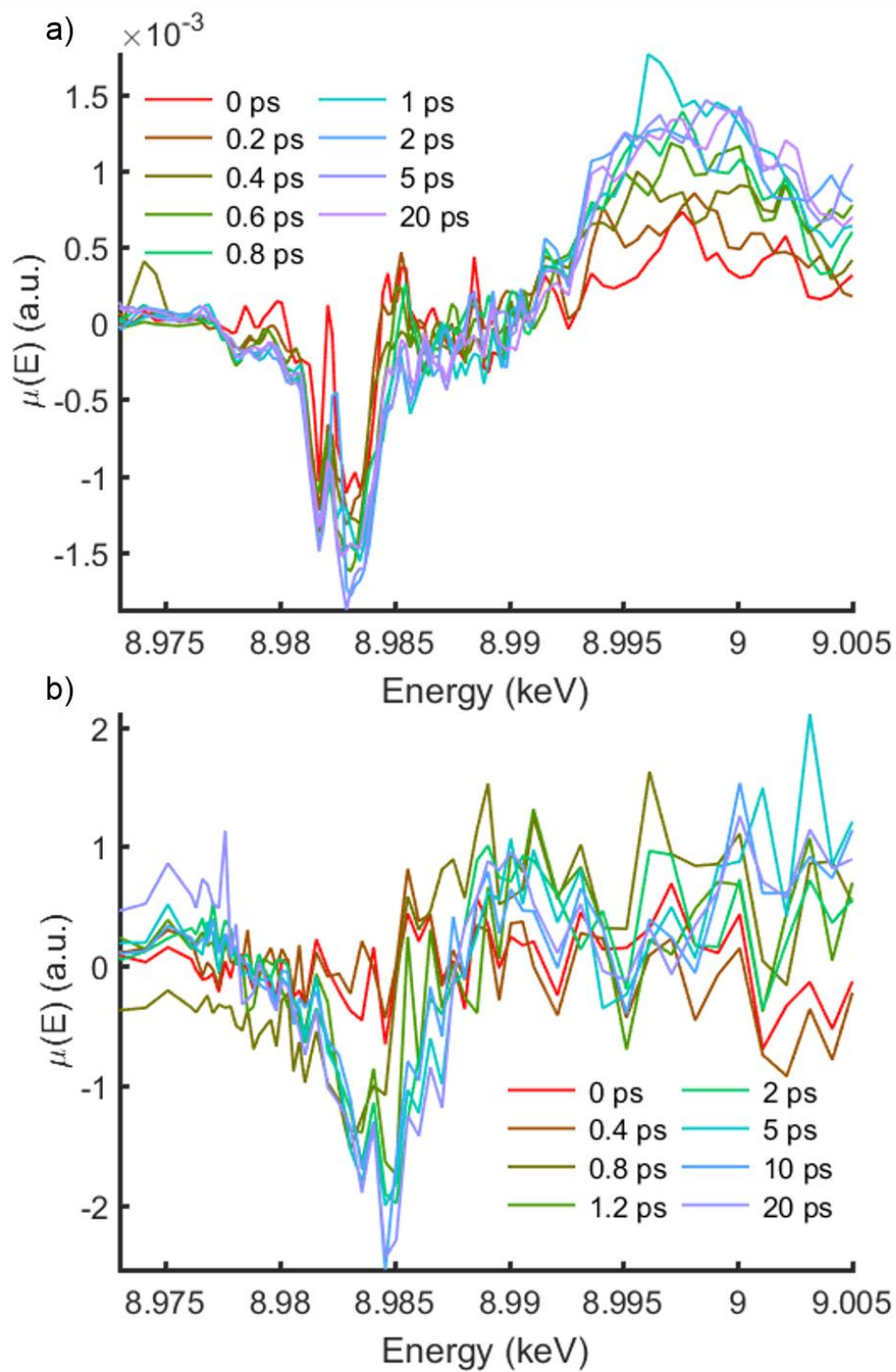


Table S1. Tabulated energies and oscillator strengths (combined dipole, magnetic dipole, and electric quadrupole transition strengths) from TDDFT UV-visible absorption calculations for [Cu(I)(dmp)₂]⁺ in its ground state geometry

Wavelength (nm)	Oscillator Strength
562.5	0.00000065594677
536.7	0.00000040435250
485.5	0.19244403780621
492.5	0.00008695097818
483.2	0.00008276327639
475.8	0.01952491350145
467.3	0.01858786306282
424.1	0.00034776339663
435.2	0.00062986755912
418.2	0.00053871956411

Table S2. Tabulated energies and oscillator strengths (combined dipole, magnetic dipole, and electric quadrupole transition strengths) from TDDFT UV-visible absorption calculations for [Cu(I)(dmp)₂]⁺ in its flattened state geometry

Wavelength (nm)	Oscillator Strength
752.4	0.03088356466103
672.2	0.01696919737496
610.4	0.00736610777641
589.2	0.00656251578031
467.9	0.16906590900101
452.8	0.00127460594367
422.1	0.00008543804265
408.8	0.00164891343478
410.8	0.00100134293465
406.2	0.00811064528887

Table S3. Tabulated energies and oscillator strengths (combined dipole, magnetic dipole, and electric quadrupole transition strengths) from TDDFT UV-visible absorption calculations for $[\text{Cu}(\text{I})(\text{dmp})_2]^+$ when it has flattened by only five degrees from the ground state.

Wavelength (nm)	Oscillator Strength
535.5	0.008276553
510.9	0.003790514
473.1	0.176753099
456.2	0.003959153
449.7	0.004648292
425.2	0.015902523
421.6	0.014594617
415.5	0.000000124
412.9	0.000493729
403.7	0.000490957

Table S4. Tabulated energies and oscillator strengths (combined dipole, magnetic dipole, and electric quadrupole transition strengths) from TDDFT UV-visible absorption calculations for [Cu(I)(dpps)₂]⁺ in its ground state geometry

Wavelength (nm)	Oscillator Strength
556.3	0.00103131616105
528.1	0.00380032544721
507.6	0.02212326563929
505.8	0.02377172539806
487.9	0.01029484657773
480.8	0.01505178863703
487.0	0.01406389109299
447.8	0.00135453579831
424.3	0.00079233871427
413.7	0.00065620897915

Table S5. Tabulated energies and oscillator strengths (combined dipole, magnetic dipole, and electric quadrupole transition strengths) from TDDFT UV-visible absorption calculations for [Cu(I)(dpps)₂]⁺ in its lowest triplet state geometry

Wavelength (nm)	Oscillator Strength
738.3	0.00672894524599
586.8	0.00985431613361
537.7	0.04739147400990
553.7	0.01715153386683
469.1	0.02101033907025
470.7	0.00195895831776
445.2	0.02148350772221
438.4	0.00835063030623
432.5	0.00200608623754
433.2	0.00687941948066